

# **Delignification of olive tree pruning using a ternary eutectic solvent for enhanced saccharification and isolation of a unique lignin fraction**

*Irene Gómez-Cruz<sup>a,b</sup>, Nalin Seixas<sup>a</sup>, Jalel Labidi<sup>c</sup>, Eulogio Castro<sup>b</sup>, Armando J.D.*

*Silvestre<sup>a</sup>, André M. da Costa Lopes<sup>a,d\*</sup>*

<sup>a</sup>CICECO, Aveiro Institute of Materials, Department of Chemistry, University of Aveiro, 3810-193 Aveiro, Portugal.

<sup>b</sup>Department of Chemical, Environmental and Materials Engineering, Universidad de Jaén, Campus Las Lagunillas, 23071 Jaén, Spain.

<sup>c</sup>Department of Chemical and Environmental Engineering, University of the Basque Country UPV/EHU, Plaza Europa 1, 20018 Donostia-San Sebastian, Gipuzkoa, Spain.

<sup>d</sup>CECOLAB, Collaborative Laboratory Towards Circular Economy, R. Nossa Senhora da Conceição, 3405-155 Oliveira do Hospital, Portugal.

\*Corresponding author: [andremcl@ua.pt](mailto:andremcl@ua.pt)

## ABSTRACT

This work aimed at exploring the potentialities of eutectic solvents (ES) in the fractionation of olive tree pruning (OTP) biomass within a biorefinery framework, targeting an efficient separation of cellulose fibers and lignin and simultaneously producing high quality fractions for further processing and application. In this sense, delignification performances of cholinium chloride:ethylene glycol, ChCl:EG (1:9) and cholinium chloride:*p*-toluenesulfonic acid:ethylene glycol, ChCl:pTSA:EG (1:1:9) as binary and ternary mixtures, respectively, were first evaluated. ChCl:EG demonstrated low efficacy for biomass delignification, while the highest lignin extraction (62.7 %) was achieved with ChCl:pTSA:EG at 80 °C and 4 h, roughly triplicating the cellulose content (62.5 %) in the resulting solid fraction compared to the raw OTP (22.3 %). This ternary ES enabled OTP matrix breakdown, which combined with lignin extraction, enhanced afterwards the enzymatic hydrolysis of cellulose-rich fraction to a maximum saccharification yield of 81.8 %. The sample exhibited an impressive aliphatic OH group content of 5.2 mmol·g<sup>-1</sup> lignin, one of the highest values amongst the state-of-the-art. The resulting phenomenon is explained by the ethylene glycol grafting onto lignin structure (aliphatic region) as demonstrated by <sup>31</sup>P and HSQC NMR, giving chemical functionality to the isolated lignin fraction. Finally, up to 90 % of the initial mass of ChCl:pTSA:EG was recovered through adsorption of impurities. NMR data validated the high purity and the same molar ratio (1:1:9) of recovered ES, two important outcomes to ensure a sustainable reutilization of this solvent.

**KEYWORDS:** delignification; eutectic solvents; lignin; functionality; solvent recovery; biorefinery; sustainability.

## 1. INTRODUCTION

Addressing the depletion of fossil fuels, the transition to renewable alternatives, and mitigating the repercussions of conventional industrial practices, represent a significant global challenge across environmental, social, and economic pillars that needs to be overcome.<sup>1</sup> In this regard, using lignocellulosic biomass as renewable raw material, whose annual production is approximately  $1 \times 10^{11}$  tons,<sup>2</sup> would allow a more sustainable model of development by partially replacing petrochemical resources for the production of clean and sustainable energy, fuels, chemicals and materials.<sup>3</sup>

Olive tree pruning (OTP) constitutes one of the main agricultural residues in Mediterranean countries generated during the removal of unproductive branches from olive groves.<sup>4</sup> OTP is a lignocellulosic material composed of cellulose (21-23 %), hemicelluloses (14-18 %) and lignin (18-23 %),<sup>5</sup> three valuable components, whose integral fractionation and conversion is required for the development of a lignocellulosic biorefinery within a circular economy perspective.<sup>6</sup> Over the years, cellulose fibers and hemicelluloses have been the target component for the production of commodities, such as biomaterials (e.g. paper and cardboards), biofuels (e.g. ethanol) and biochemicals<sup>7,8</sup> with commercial profitability.<sup>9</sup> However, low or negligible attention has been given to the valorization of lignin. For a more sustainable management of biomass as material resource, lignin isolation and further conversion towards biochemicals and biomaterials is required, alongside with the carbohydrate fraction in the frame of a biorefinery scheme.

Lignin is a heterogeneous, amorphous and aromatic polymer with interesting physicochemical functionalities that deserve strategical exploitation.<sup>10</sup> It is an amorphous macromolecular structure mainly composed of three monolignol structures, namely I-coumaryl, coniferyl, and sinapyl alcohols, which linked by ether ( $\beta$ -O-4,  $\alpha$ -O-4, 4-O-5) and

carbon-carbon (5-5',  $\beta$ -5,  $\beta$ -1,  $\beta$ - $\beta$ ) bonds during lignin biosynthesis giving rise to *p*-hydroxyphenyl (H), guaiacyl (G), and syringyl (S) units, respectively.<sup>11</sup> Lignin is thus an ubiquitous material that exhibit high thermal stability, biodegradability, antioxidant activity, amphiphilicity, reinforcing capacity, UV protecting ability, among other valuable properties<sup>12,13</sup> with high potential for multiple applications in the biofuels, and biobased materials and chemicals sectors.<sup>14</sup>

Several authors have reported OTP delignification mediated by traditional methodologies, such as organosolv treatment with ethanol,<sup>15</sup> acetosolv and formosolv treatments with acetic acid and formic acid, respectively,<sup>16</sup> soda/anthraquinone extraction,<sup>17</sup> water<sup>18</sup> and steam explosion with phosphoric acid.<sup>19</sup> The common denominator in their development relies on the maximum disruption of biomass matrix and exposure of the carbohydrate fraction towards enzymatic hydrolysis and biotechnological fermentation. However, the high severity of those processes brings technical limitations related to the formation of unproductive furfural and HMF, two main inhibitors for microorganism fermentation, as well as economic concerns associated to the energetic demand and specific equipment requirement. Furthermore, lignin removal is mandatory in those processes, but any kind of valorization for this macromolecular component is considered. Generally, lignin obtained from these processes exhibit a high degree of degradation (condensation) in its macromolecular structure, decreasing its chemical functionality for application. If these undesired reactions are prevented, lignin will be more prone for upstream conversion into biobased chemicals and materials.

Therefore, deploying efficient and environmentally friendly biomass delignification processes, allowing not only carbohydrate exposure to enzymatic hydrolysis, but also enabling the isolation of lignin with reduced condensation structures, or in the best scenario,

imparting new chemical functionalities to isolated lignin, is highly required for the implementation of next generation biorefineries processes.<sup>20</sup> In this context, eutectic solvents (ES), a neoteric class of green solvents, may provide a reliable solution to improve the sustainability of biomass processing, particularly in the fractionation performance.

ES are mixtures of hydrogen bond donor (HBD) and hydrogen bond acceptors (HBA) species that exhibit lower melting points than each of the individual components.<sup>21</sup> ES exhibit important properties to reach process sustainability, including low toxicity, simple preparation, low cost, biodegradability, recyclability and high solubility power and thermal stability.<sup>22</sup> These features make them an environmentally friendly alternative to conventional organic solvents.<sup>7,23</sup> The state-of-the-art discloses that these solvents are able to solubilize lignin (e.g. Kraft and Organosolv lignins)<sup>24</sup> to the detriment of a poor performance for cellulose dissolution, which is an important trigger to reach enhanced biomass fractionation.<sup>9</sup> Moreover, ES have shown to provide favorable physicochemical properties to the extracted lignin, for instance, by maintaining a high degree of  $\beta$ -O-4 aryl ether bonds in lignin structure<sup>7</sup>, when operated at low temperature (<100 °C).

In particular, ChCl:LA has demonstrated high performance in biomass delignification, particularly at higher LA molar ratios.<sup>25</sup> In this case, the delignification mechanism relies on the partial acidic cleavage of  $\beta$ -O-4 bonds promoted by the acid component of the ES, and catalytically boosted by the halide from cholinium salt.<sup>26</sup> However, excess of organic acid combined with temperatures higher than 100 °C demonstrated a negative impact on lignin chemical structure, increasing the content of condensed structures.

On the other hand, ES containing alcohols, such as ethylene glycol (EG) or glycerol, exhibit high capacity for lignin dissolution (technical lignins)<sup>23</sup> low corrosivity and biocompatibility

with subsequent downstream processing (enzymes and microorganisms). However, these alcohol-based ES have revealed low efficacy in disrupting the lignocellulosic biomass matrix, including cleavage of lignin chemical bonds, and consequently they have shown low efficiency in extracting lignin from biomass. In this sense, a ternary system comprising a wise combination of acid and alcohol, besides the presence of ChCl may provide benefits in the fractionation of carbohydrate and lignin, since it will offer simultaneous acidic catalytic conditions and solvent power in a single solvent formulation. A previous study demonstrated that ternary ES consisting of ChCl:LA:EG, although enabling a good pre-treatment performance of rice straw, improving the digestibility of polysaccharides and increasing the biobutanol titer by fermentation, was ineffective in extracting lignin.<sup>27</sup> To overcome this limited fractionation, *p*-toluenesulfonic acid (pTSA) is proposed in the present study as the acid component of ES, since, based on data reported elsewhere,<sup>26</sup> it may induce better acidic catalytic cleavage conditions than the LA counterpart. Moreover, due to its aromatic structure and hydrotropic properties, pTSA may improve even more the dissolution process of the amphiphilic lignin macromolecules.<sup>28,29</sup>

In this sense, this study aimed at evaluating the efficiency of OTP delignification with EG-based ES, namely the ternary ChCl:pTSA:EG (1:1:9) and the binary ChCl:EG (1:9) (for comparison). The fractionation performance of ChCl:pTSA:EG was assessed, particularly on the quality of cellulose and lignin as isolated fractions. The isolated cellulose-rich solid was morphologically and chemically characterized to evaluate the effect of ternary ES, while a saccharification step was subsequently appraised towards the production of fermentable sugars. On the other hand, the lignin-rich fraction was extensively characterized by FTIR, 2D HSQC and <sup>31</sup>P NMR, elemental analysis, TGA and GPC to inspect its physicochemical characteristics and to infer its reactivity with ternary ES. Finally, a proof-of-concept upon ES

recycling was performed by adsorption of impurities to ensure the sustainability of the process.

## **2. EXPERIMENTAL SECTION**

### **2.1. Materials**

Olive tree pruning (OTP) was obtained from an olive grove in the province of Jaén (Spain) after fruit harvesting. OTP was dried at room temperature and milled with a Retsch SM 100 blade mill (Haan, Germany) to particle size 1 to 8 mm before its use. Then, OTP was milled to ~1 mm size using an ultracentrifugal ball mill ZM 200 (Retsch, Haan, Germany) and sieved to a particle size between 0.250-1 mm. Afterwards, the moisture content of the biomass was determined to  $6.56 \pm 0.07$  %, using the HE53 moisture analyzer (Mettler Toledo, Barcelona, Spain). Finally, OTP chemical composition was determined by the analytical methods of the National Renewable Energy Laboratory (NREL, Golden, CO, USA).<sup>30</sup>

### **2.2. Eutectic solvents preparation**

The binary ES was prepared by mixing ChCl with EG in a molar ratio of 1:9 (ChCl:EG), while ChCl, pTSA and EG were used in a molar ratio of 1:1:9 to prepare the ternary ES. For the formulation of both ES, the moisture content of the different precursors was measured by Karl Fischer coulometric titration (Metrohm 831, Herisau, Switzerland). Each mixture was melted in sealed glass flasks in an oil bath (maximum temperature 80 °C) for 1 h with constant magnetic stirring until a homogeneous liquid was obtained. Finally, both mixtures were stored at room temperature until use.

### 2.3. Biomass fractionation process

The experimental procedure for the delignification of OTP is shown in Figure 1. Briefly, 1 g of dry biomass was added to the reaction glass tube together with the ES solution (9 g total) to achieve a dry solid loading of 10 % by weight. The reaction tubes were sealed and incubated in a Radleys Tech carousel system (Saffron Walden, UK) magnetically stirred at 500 rpm. Binary ES extractions were performed at 80, 100 and 120 °C and residence times of 0.5, 1 and 2 h, while ternary ES tests were carried out at a fixed temperature of 80 °C and the extraction time was varied from 0.5 to 6 h.

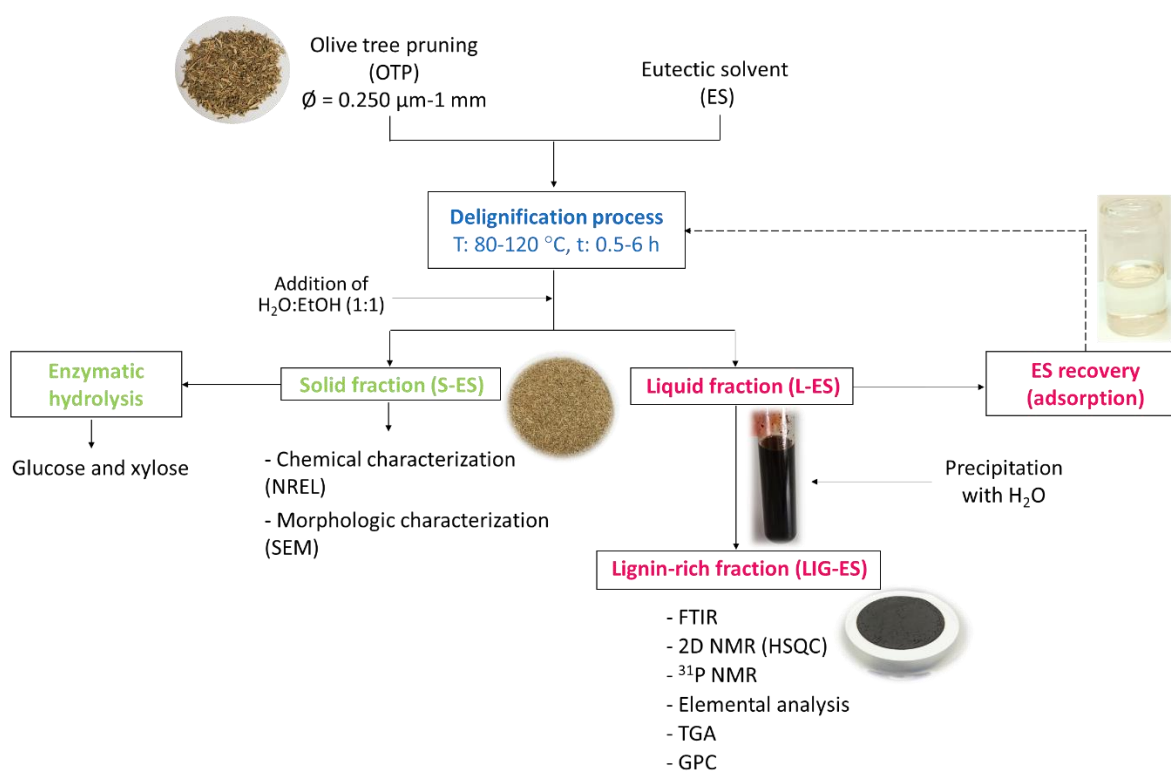


**Figure 1.** Scheme of the OTP fractionation developed in this study using eutectic solvents.

After biomass delignification, the tubes were cooled down and 20 g of water:ethanol (1:1 v/v) was added to the reaction tube to reduce the viscosity of resulting liquid solution, while maintaining soluble the extracted biomass components.

The liquid and solid fractions were separated in a vacuum filtration system equipped with 0.45  $\mu\text{m}$  porosity Cytiva Whatman nylon membrane filters (Fisher Scientific, Pittsburgh, PA, USA). The solid fraction (S-ES) was thoroughly washed with distilled water to remove ES residues and dried in an oven at 40 °C for 24 h. Subsequently, it was weighed to determine the solid recovery according to equation (1):

$$\text{Solid recovery (\%)} = \frac{\text{Delignified solid fraction weight (g)}}{\text{Raw biomass weight (g)}} \cdot 100 \quad (1)$$

For lignin isolation, 20 mL of liquid fraction (L-ES) was gradually poured into a tube half-filled with ice to promote precipitation of the extracted lignin and then 40 mL of distilled water was added. The obtained solution was stored at 4 °C for 24 h to ensure maximum lignin precipitation. The lignin-rich fraction (LIG-ES) was then filtered using vacuum filtration system as mentioned before, washed with 50 mL of distilled water and dried at 40 °C for 24 h.

Delignification yield, isolated lignin and selectivity were calculated based on equations (2) and (3), respectively:

$$\text{Delignification yield (\%)} = 1 - \frac{\text{Lignin content in delignified solid fraction (g)}}{\text{Lignin content in raw biomass (g)}} \cdot 100 \quad (2)$$

$$\text{Isolated lignin (mg lignin} \cdot \text{g}^{-1} \text{ biomass)} = \frac{\text{Precipitated ligin weight (mg)}}{\text{Raw biomass weight (g)}} \quad (3)$$

Subsequently, isolated lignin fraction was characterized to determine its structural composition by different analytical techniques as described in Section 2.6.

#### **2.4. Enzymatic hydrolysis of the solid fraction**

OTP and S-ES obtained after extraction with ternary ES at 80 °C for 4 h were used as substrates for enzymatic hydrolysis (EH). The commercial enzyme solution Cellic® CTec2 (Novozymes A/S, Bagsværd, Denmark) at 15 filter paper units (FPU)/g substrate and  $\beta$ -glucosidase (Novozymes A/S, Bagsværd, Denmark) at 15 international units (IU)/g substrate were used to hydrolyze the aforementioned solids. The S/L ratio used was 5% w/v, citric acid-citrate buffer 0.05 M at pH 4.8 and Avicel® PH-101 (Sigma-Aldrich, St. Louis, MO, USA) was used as enzymatic control. The samples were processed on an orbital shaker (IKA KS 4000 i control, Staufen, Germany) for 72 h at 50 °C and 150 rpm. Samples were taken at 8, 24, 32, 48 and 72 h, and the released glucose and xylose concentrations were determined by HPLC-RID analysis as detailed in section 2.5. Enzymatic digestibility ( $Y_{WIS}$ ) and enzymatic hydrolysis yield (EH yield) were calculated as follows:

$$Y_{WIS} (\%) = \frac{g \text{ glucan by EH}}{100 g \text{ glucan in S-ES}} \quad (4)$$

$$EH \text{ yield } (\%) = \frac{g \text{ glucan by EH}}{100 g \text{ glucan in OTP}} \quad (5)$$

#### **2.5. Recovery of ternary ES**

The recovery of the ternary ES (ChCl:pTSA:EG) after OTP delignification was performed by adsorption using C18 reversed-phase silica gel (LiChroprep® RP-18, Merck Millipore,

Burlington, MA, USA) stationary phase and a Fisherbrand™ GP 1000 peristaltic pump (Thermo Scientific Chemicals, Waltham, MA, USA) to favor the elution process.

The stationary phase (30 g LiChroprep® RP-18) was activated with 400 mL of methanol and conditioned with 400 mL of distilled water. Approximately 30 mL of the L-ES (after lignin precipitation) was loaded to the column and then eluted with a large volume of distilled water to ensure maximum recovery of ES. Regeneration of the column was performed with 100 mL methanol and followed by column conditioning with water for a next chromatographic run. Finally, ES was recovered by water evaporation using a BÜCHI R-114 rotary evaporator (Thermo Scientific Chemicals, Waltham, MA, USA) and preserved in a desiccator.

## **2.6. Sample characterization**

### **2.6.1. Chemical analysis of solid fraction**

The OTP and all delignified OTP solids (S-ES) with binary and ternary ES were chemically characterized according to the standard NREL.<sup>30</sup>

In this methodology, 0.3 g of biomass is subjected to a two-step acid hydrolysis to hydrolyze and solubilize all the structural carbohydrates present. The first step uses concentrated H<sub>2</sub>SO<sub>4</sub> (72 % v/v) for 1 h at 30 °C and the second step diluted H<sub>2</sub>SO<sub>4</sub> (4 % v/v) at 121 °C for 60 min. The hydrolysates obtained were analyzed by HPLC-RID (described in section 2.5) to determine the concentration of monomeric sugars released after acid hydrolysis and the content of acetyl groups at 280 nm. The acid soluble lignin content (ASL) was determined in the liquid fraction by UV/VIS using a spectrophotometer (UV-1700 PharmaSpec Shimadzu, Kyoto, Japan) measuring at 240 nm wavelength.

Finally, acid insoluble lignin (AIL) and acid insoluble ash contents (575 °C, 6 h) were determined by gravimetric analysis by weighing the solid resulting from two-step acid hydrolysis.

#### 2.6.2. Morphological analysis of solid fraction

Scanning electron microscopy (SEM) was used to examine the morphological changes of the biomass before (raw OTP) and after delignification (S-ES) with ternary ES at 80 °C for 4 h. Dry samples were fixed with double-sided carbon adhesive tape mounted on SEM grids and coated with carbon before SEM analysis. The images were acquired at high vacuum conditions, 15 kV and 30x, 200x and 500x magnification using a Hitachi SU-70, Tokyo, Japan instrument.

#### 2.6.3. Liquid fraction characterization

The L-ES was analyzed by HPLC-PAD (Elite LaChrom VWR HITACHI, Tokyo, Japan) to determine the content of sugars and sugar degradation products (furfural and HMF). The samples (10 µL) were injected into the HPLC system consisting of a pump L-2130 (Hitachi, Chiyoda, Japan), an autosampler L-2200 (Hitachi, Chiyoda, Japan) and two detectors, a photodiode array detector (PAD) L-2455 (Hitachi, Chiyoda, Japan) and a refractive index (RI) detector L-2490 (Hitachi, Chiyoda, Japan). The compounds were separated on a Rezex ROA-Organic acid H<sup>+</sup> 8% ion exchange column (300 x 7.8 mm; particle size 8 µm), supplied by Phenomenex (Torrance, CA, USA) and maintained at 65 °C (Gecko 2000 oven, CIL Cluzeau, Sainte-Foy-la-Grande, France). The eluent used was a 0.005 N solution of sulfuric acid at a flow rate of 0.5 mL·min<sup>-1</sup>. Calibration curves of glucose, xylose, furfural and HMF were used to determine the concentration of the analytes in the obtained liquid samples.

#### 2.6.4. FTIR-ATR analysis of lignin

FTIR-ATR analysis of the LIG-ES sample and Kraft lignin (as a reference) was carried out on a PerkinElmer Spectrum BX spectrometer (Waltham, MA, USA) coupled with an attenuated total reflection (ATR) Golden Gate horizontal cell and an internal diamond crystal. Each spectrum corresponded to the average of 32 scans in absorbance units and was recorded in the region between 4000 and 400  $\text{cm}^{-1}$  with a resolution of 4  $\text{cm}^{-1}$  and interval of 1  $\text{cm}^{-1}$ . For the subsequent analysis, baseline correction and normalization of spectra were performed.

#### 2.6.5. $^1\text{H}$ and $^{13}\text{C}$ NMR analysis

The  $^1\text{H}$  and  $^{13}\text{C}$  NMR spectra of pristine and recovered ternary ES were recorded at 300.13 MHz and 75.47 MHz, respectively, using a Bruker AVANCE 300 MHz NMR (Bruker, Billerica, MA). The ternary ES was appropriately dissolved in deuterated water ( $\text{D}_2\text{O}$ ) (20 mg/500  $\mu\text{l}$  of solvent) and the mixture was transferred to a 5 mm diameter NMR tube (Wilmad-LabGlass<sup>TM</sup>, Vineland, USA).

#### 2.6.6. 2D HSQC NMR analysis

For the analysis, 55 mg of LIG-ES sample was dissolved in 0.5 mL of  $\text{DMSO-}d_6$ . The resulting mixture was then carefully added to a 500 MHz NMR tube (Wilmad-LabGlass, Vineland, NJ, USA). A Bruker AVANCE 500 MHz NMR spectrometer (Bruker, Billerica, MA) was used to acquire the two-dimensional  $^1\text{H}$ - $^{13}\text{C}$  chemical shift ( $\delta\text{H}$  0 ppm – 9 ppm and  $\delta\text{C}$  0 ppm -180 ppm) correlations. The system was equipped with a 5 mm TXI  $^1\text{H}/^{13}\text{C}/^{15}\text{N}$  cryoprobe inverse gradient using the "hsqcetgp" pulse sequence supplied by Bruker with 2D

H-1/X correlation using inept double transfer (fitting pulses), Echo/Antiecho-TPPI gradient selection for improved phase sensitivity and decoupling during acquisition. Chemical shifts were calibrated with reference to the center peak of the solvent DMSO-D<sub>6</sub> ( $\delta$ H 2.49 ppm and  $\delta$ C 39.5 ppm). Experimental conditions were: temperature of 25 °C, spectral width of 11 ppm and 165 ppm in the F2 (<sup>1</sup>H) and F1 (<sup>13</sup>C) dimension, respectively, 194 scans, 1024 data points and a recycle delay of 1.5 s.

Lignin correlation signals in the HSQC spectrum of the LIG-ES were assigned according to the literature.<sup>17,19,23,31</sup>

#### 2.6.7. <sup>31</sup>P NMR analysis

A solvent mixture of anhydrous pyridine and deuterated chloroform (1.6:1 v/v) was prepared and protected from moisture with molecular sieves (5Å). An internal standard (IS) solution was then prepared using the solvent mixture and adding chromium (III) acetylacetonate (3.6 mg·mL<sup>-1</sup>) and cyclohexanol (20 mg·mL<sup>-1</sup>) as the relaxation reagent and the IS, respectively. About 30 mg of the lignin sample, previously dried at 40 °C for 6 h in a vacuum oven (Thermo Scientific VT 6025, Waltham, MA, USA), was weighed into a vial. The sample was then dissolved in a 500  $\mu$ L aliquot of the solvent mixture and a 100  $\mu$ L aliquot of IS solution. After thorough stirring, 100  $\mu$ L TMDP was added to the above solution, and the mixture was again stirred before transferring to an NMR tube (Wilmad-LabGlass, Vineland, NJ, USA) for further analysis. Finally, the <sup>31</sup>P NMR spectra were acquired with a Bruker AVANCE 400 MHz NMR spectrometer (Billerica, MA, USA) and the quantification of different type of hydroxyl groups was carried out according to equation (6):

$$\text{Functional group (mmol/g lignin)} = \frac{\text{normalized peak area}}{\text{sample weight}} \cdot \text{IS concentration} \cdot 0.1 \quad (6)$$

#### 2.6.8. Thermogravimetric analysis

A Shimadzu TGA-50 Series analyzer (Shimadzu Corporation, Kyoto, Japan) was used for thermogravimetric analysis (TGA) of LIG-ES samples. For this analysis, ~5 mg of sample was placed in an aluminum container and analyzed at constant nitrogen flow rate of 50 mL·min<sup>-1</sup>. The samples were heated at a rate of 10 °C·min<sup>-1</sup> within a temperature range of 25-800 °C.

#### 2.6.9. Experimental and analytical error

All the experiments were performed in triplicate and the obtained results were expressed as means with associated standard deviation ( $\sigma$ ). The applied temperature in the reactions demonstrated a  $\Delta(T) = 1$  °C. All the mass determinations were performed with a given  $\Delta(m) = 0.1$  mg.

### 3. RESULTS AND DISCUSSION

#### 3.1. Evaluation of OTP delignification process with examined ES

##### 3.1.1. Solid and liquid composition

The determined chemical composition of raw OTP on dry basis exhibited 22.3 % glucan, 15.5 % hemicelluloses, 18.2 % lignin, 4.3 % ash and 31.3 % others (e.g. free sugars, phenolic compounds, proteins, lipids, among others). These values were taken as a basis for comparison with the solid recovery yield and chemical composition of the solid fractions (S-ES) obtained after OTP delignification with binary ES (ChCl:EG; 1:9) and ternary ES

(ChCl:pTSA:EG; 1:1:9) as depicted in Figure 2a and 2b, respectively. The composition of S-ES without reference on dried OTP is shown in Figure S1.

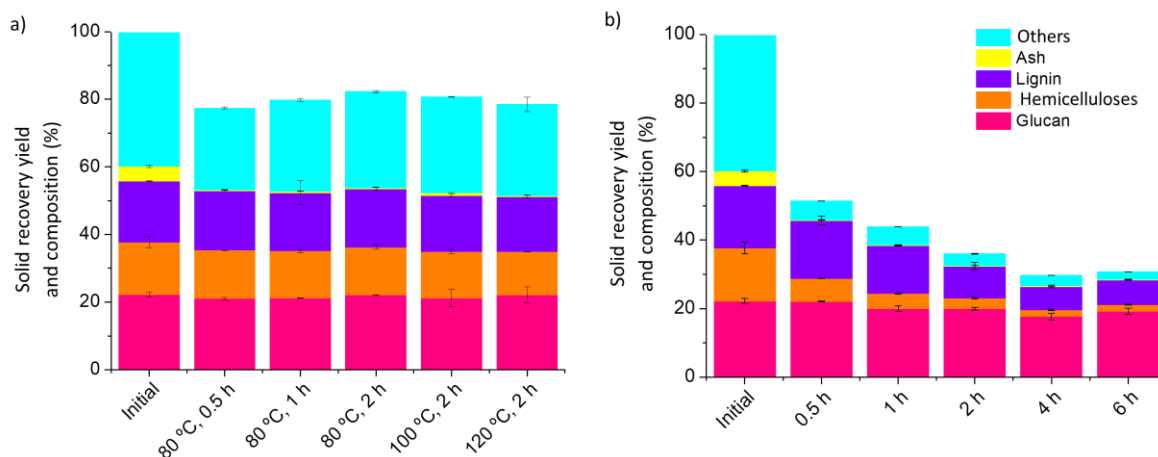


**Figure 2.** Solid recovery yield (total bar) and composition of main fractions (stacked bars) after OTP treatment with a) ChCl:EG and b) ChCl:pTSA:EG. Composition based on dried raw OTP.

The application of binary ES (ChCl:EG; 1:9) exhibited no relevant effect on the S-ES composition at the examined temperatures and times (Figure 2a and Figure S1a). The relative proportions of cellulose, hemicelluloses and lignin contents were kept practically constant over the studied conditions (compared to raw OTP composition), with the exception of the sample obtained under the most severe conditions (120 °C, 2 h) where 10.7 % lignin removal and solubilization of 11.1 % hemicelluloses was achieved. In literature, the same binary ES also enabled low hemicelluloses and lignin extraction yields from pine wood (2.7 % and 4.8 %, respectively)<sup>32</sup> and bamboo wood (8.5 % and 4.4 %, respectively).<sup>33,34</sup> The reduced delignification performance of the alcohol-based ES and consequently low biomass matrix disruption, associated with the absence of an acid catalyst is a major reason to explain these

low lignin extraction yields. Indeed, the extraction capacity of ChCl:EG relies only on the partial dissolution of “others” fraction of OTP as demonstrated in Figure 2a. In this regard, several studies have demonstrated the capacity of ChCl:EG to extract plant low molecular weight secondary metabolites, such as phenolic compounds,<sup>35,36</sup> corroborating the obtained results.

On the other hand, OTP treatment with ternary ES (ChCl:pTSA:EG), at 80 °C, showed a continuous extraction of lignin and hemicelluloses (Figure 2b) to the liquid phase (L-ES) along the treatment time, enhancing cellulose content in the obtained solid (between 43.0-62.5%; Figure S1b). With only 30 min of treatment, 51.4 % solid recovery yield was achieved, suggesting an effective biomass extracting capacity of ternary ES. The solid recovery yield decreased during treatment time to a minimum of 30.8% at the end of 4 h. Under the same conditions, maximum extraction yields of 62.7 %, 87.3 %, 92.5 % of lignin, hemicelluloses and “others” respectively were observed. Therefore, the composition of S-ES demonstrated that ChCl:pTSA:EG was highly selective for lignin, hemicelluloses and extractives removal, while preserving cellulose content in the remaining solid.<sup>32</sup> The analysis of the liquid phase, discussed in the next section also supports these conclusions.

The monosaccharide composition in the L-ES (Table S1) shows that hemicelluloses were extracted and hydrolyzed into xylose and arabinose at great extent during treatment with ternary ES. Glucose was barely produced, which means a desired low extent of cellulose hydrolysis during treatment. Surprisingly, sugar degradation compounds, including furfural and HMF, were not detected during OTP treatment with this acidic ternary ES. This suggests that the chemical environment provided by ChCl:pTSA:EG does not favor degradation of monosaccharides into corresponding furans, which is a technical advantage for the

subsequent valorization of both solid and liquid fractions in contrast to conventional acid-based treatments with mineral acids (e.g. aqueous H<sub>2</sub>SO<sub>4</sub> hydrolysis).<sup>37</sup>

### 3.1.2. Morphology of solid fraction

The morphology of S-ES sample obtained with the ternary ES at 80 °C and 4 h was also evaluated by SEM analysis to give insights on the effectiveness of ternary ES in disrupting OTP matrix (Figure 3). However, superior magnifications (200x and 500x) demonstrates that both parts are distinct between raw OTP and S-ES. The block-shaped structure in OTP relies on smooth and compact cement-like structures, represented by the intricate matrix composed of cellulose, hemicelluloses and lignin, while the same structure in S-ES depicts exposed and interlaced cellulose fibers. On the other hand, the cylindrical shapes go from a highly compact and well-organized morphology in raw OTP into disrupted and disorganized matrix in S-ES, which provides gives clear evidence of the effective biomass matrix disruption mediated by ternary ES with consequent dissolution of biomass components (lignin, hemicelluloses and extractives as mentioned before), thus leaving cellulose fibers more accessible for enzymatic hydrolysis.

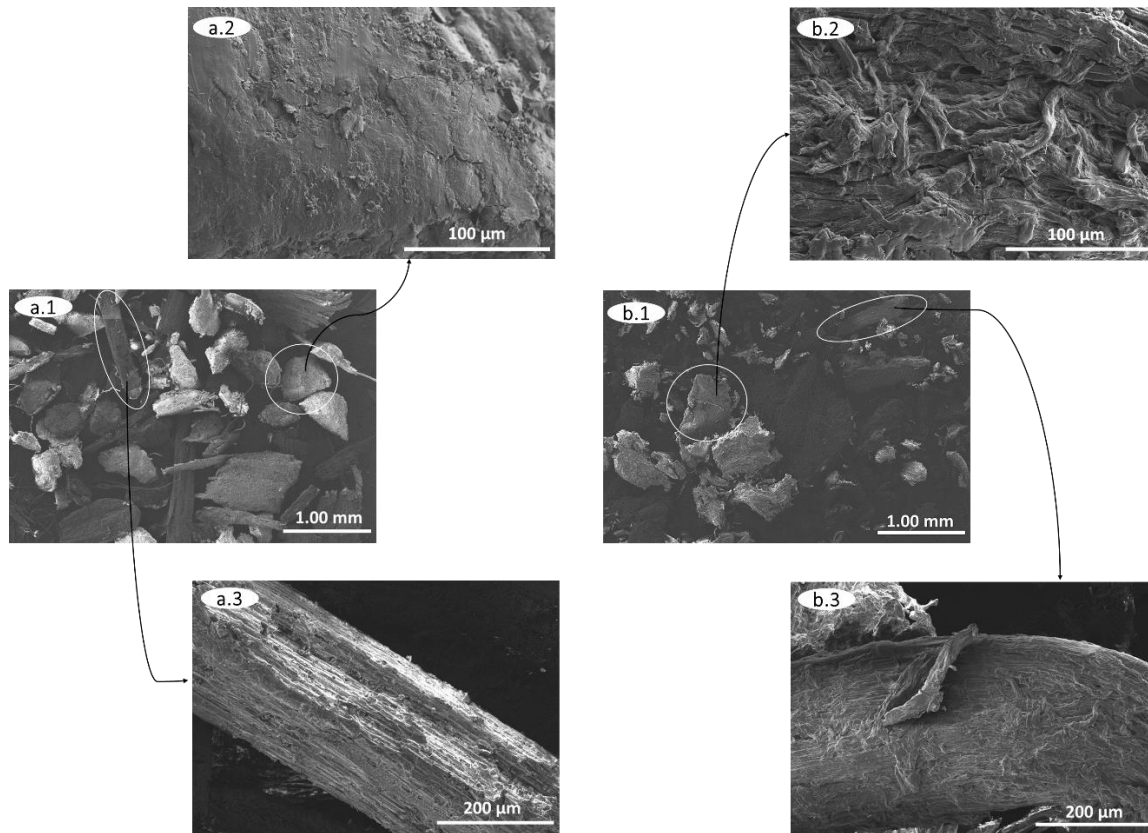


**Figure 3.** Scanning electron microscopy (SEM) images of a) raw OTP and b) S-ES fraction obtained after treatment with ternary ES at 80 °C for 4 h, at different magnifications: 30x (a1 and b1), 200x (a2 and b2) and 500x (a3 and b3).

### 3.1.3. Enzymatic saccharification of solid fraction

The digestibility of the S-ES sample (80 °C and 4 h) into fermentable sugars was also investigated. Figure 4 shows the enzymatic digestibility ( $Y_{WIS}$ ) expressed as  $g \text{ glucan} \cdot 100 g^{-1} \text{ glucan}$  in S-ES and the enzymatic hydrolysis yield (EH yield) referred to  $g \text{ glucan} \cdot 100 g^{-1} \text{ glucan}$  in OTP.

As expected OTP showed a very low  $Y_{WIS}$  ( $30.2\% - g_{\text{glucan}} \cdot 100 g^{-1}_{\text{glucan S-ES}}$ ), caused by the intricate matrix of the material and the presence of enzyme inhibitors, such as compounds associated to “others” fraction (31.3% content in OTP) and lignin as observed in SEM images

(Figure 3).<sup>38</sup> The last might adsorb to enzyme surface<sup>39</sup> or act as a physical barrier impeding enzymes to access cellulose fibers,<sup>40</sup> and thus leading to low saccharification yields.

On the other hand, S-ES presented a  $Y_{WIS}$  near 100 % ( $\text{g}_{\text{glucan}} \cdot 100 \text{ g}^{-1}_{\text{glucan in S-ES}}$ ), indicating that almost complete conversion of cellulose from the solid delignified with ternary ES at 80 °C and 4 h was achieved. In addition, an EH yield of 81.8 % ( $\text{g}_{\text{glucan}} \cdot 100 \text{ g}^{-1}_{\text{glucan OTP}}$ ) was obtained, 63 % higher than that of untreated OTP. This result confirms that OTP fractionation with ternary ES produced a cellulose-rich fraction more accessible to cellulolytic enzymes.

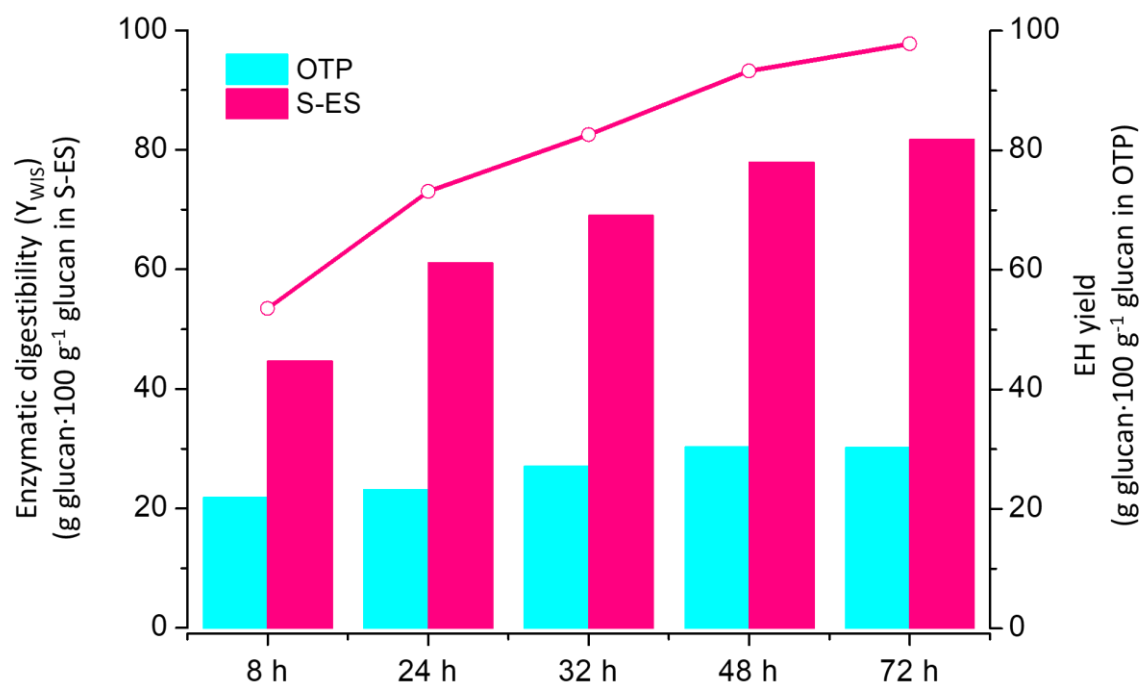


**Figure 4.** Enzymatic digestibility ( $Y_{WIS}$ ) and enzymatic hydrolysis yield (EH yield) of OTP and S-ES (80 °C, 4 h).  $Y_{WIS}$  (lines) and EH yield (bars).

### 3.2. Delignification efficiency of ES and isolation of lignin

Apart from the valorization of the cellulose-rich fraction, targeting an efficient delignification and subsequent isolation of lignin is required in developing biomass fractionation processes. In this regard, the delignification yield and subsequent lignin precipitation yield were evaluated for both binary and ternary ES.

The biomass delignification yields followed the same trends observed in the discussion of S-ES chemical composition. The binary ES was ineffective in extracting lignin from OTP, since delignification yield poorly increased from 80 °C (5.36 %) to 120 °C (10.73 %) for 2 h of treatment (Table S2 in SI). On the other hand, the ternary ES improved considerably the delignification yield with increasing extraction time up to 4 h (62.7%), reaching at the same period the highest lignin precipitation yield (74.6 mg lignin·g<sup>-1</sup> biomass) (Table 1).

**Table 1.** Delignification yield (%) and LIG-ES (mg lignin·g<sup>-1</sup> biomass) mediated by the ChCl:pTSA:EG eutectic solvent.

Time (h)	Delignification yield (%)	Isolated lignin (mg lignin·g <sup>-1</sup> biomass)
0.5	7.4 ± 3.4	29.1 ± 0.5
1	23.2 ± 2.3	36.3 ± 0.7
2	48.7 ± 2.6	54.9 ± 6.5
4	62.7 ± 1.9	74.6 ± 0.4
6	60.1 ± 1.4	71.9 ± 1.6

When contrasting to ChCl:EG, the higher OTP delignification with ChCl:pTSA:EG due to the presence of pTSA, which catalyzes the acidic disrupting chemical bonds of lignocellulosic biomass components, and particularly ether bonds in lignin structure, ether bonds between lignin-polysaccharide, inducing delignification, and as an unwanted reaction

glycosidic bonds in polysaccharides.<sup>41</sup> Although at different molar ratios, ChCl:pTSA:EG has been also explored in the delignification of other lignocellulosic biomasses, such as bamboo<sup>34</sup> and switchgrass.<sup>42</sup> For instance, at molar ratio 1:1:0.5, this ternary ES showed a very high bamboo delignification (71 %),<sup>34</sup> while using switchgrass and same ES at molar ratio 1:1.9:0.1 approximately 91 % delignification was achieved.<sup>42</sup> These might, be seen as better than those presented in this study, however, they are associated to the delignification of less recalcitrant starting materials (switchgrass and bamboo), and also worth mentioning higher temperatures were used (120 °C in both cases). Yet, the mild temperature used in this work (80 °C) is expected to become a bonus to the characteristics of extracted lignin. For example, by providing less condensed structures and subsequently increased number of functional groups to lignin macromolecular structure, which in turn, exhibits reactivity in subsequent valorization steps. Indeed, elucidating the structural characteristics of lignin provides useful information upon possible applications. This will be discussed below.

Lignin isolated with ChCl:pTSA:EG (1:1:9) at the best delignification and precipitation conditions (80 °C/4 h), called as LIG-ES, was characterized by FTIR, 2D HSQC NMR, <sup>31</sup>P NMR, elemental analysis, TGA and GPC.

The FTIR spectrum of LIG-ES showed a typical fingerprint of lignin. The infrared vibrations matched those from native Kraft lignin as depicted in Figure 5 (total spectrum is shown in Figure S2). The corresponding infrared vibration assignments of lignin are disclosed in Table S2. For instance, and in agreement with literature,<sup>18,23</sup> the bands at 1327 cm<sup>-1</sup> and 1118 cm<sup>-1</sup> are assigned to S-type units, while the bands at 1212 cm<sup>-1</sup> and 1031 cm<sup>-1</sup> indicate the presence of G-type units (Figure 5 and Table S3). The band at 1090 cm<sup>-1</sup> assigned to C–O stretching<sup>43</sup> slightly appears in LIG-ES spectrum, which can be attributed to the increase of aliphatic hydroxyl groups.<sup>44</sup> In addition, the region between 1650 and 1750

$\text{cm}^{-1}$ , associated to carbonyl, ketones, carboxylic and ester groups, is apparently higher for the LIG-ES sample, which means that other compounds from OTP (fatty acids are an example) might also precipitate alongside lignin.

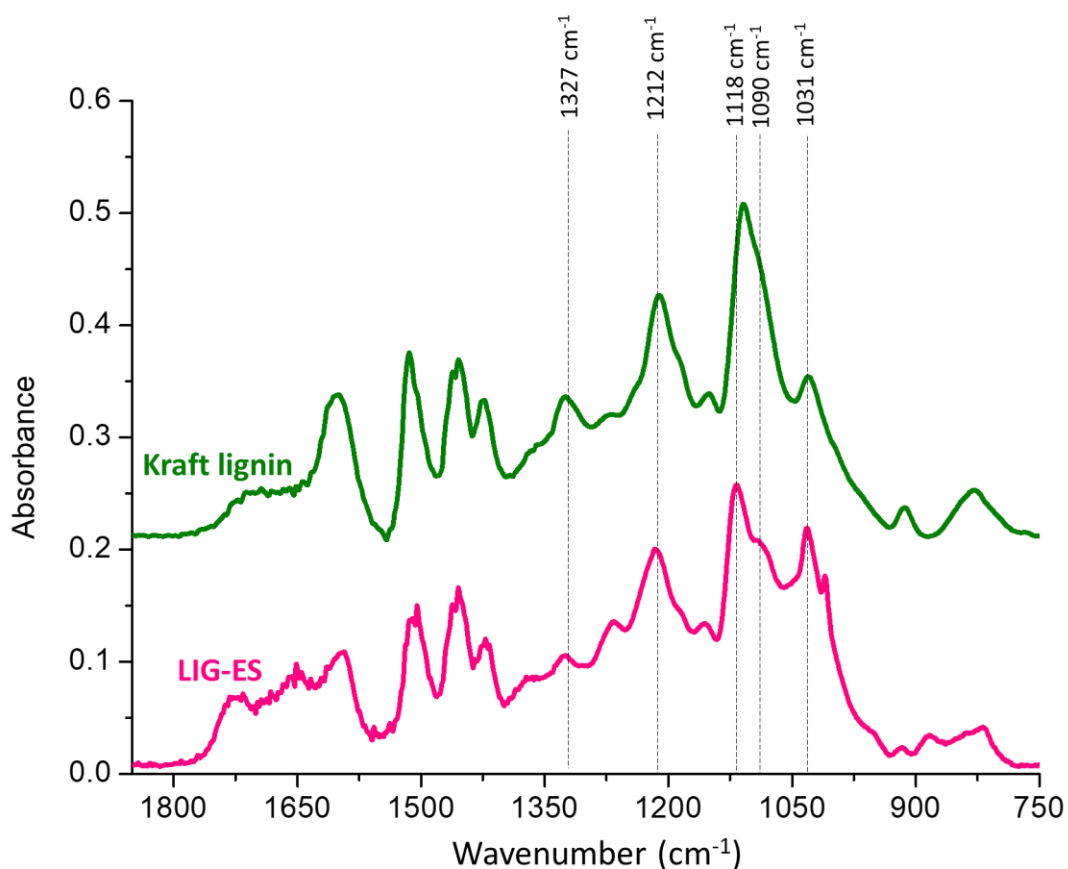


**Figure 5.** FTIR spectra (magnification of the 1850–750  $\text{cm}^{-1}$  region) of LIG-ES obtained after extraction with  $\text{ChCl:pTSA:EG}$  at 80 °C and 4 h, and of Kraft lignin (used for comparative purposes).

Nevertheless, 2D HSQC and  $^{31}\text{P}$  NMR were also performed to support FTIR data and to acquire more insights into LIG-ES chemical structure. The assigned HSQC cross signals are depicted in Figure 6 and the corresponding assignments are described in Table S4 (SI) The

HSQC data showed that the most intense correlation signals in the oxygenated aliphatic region of the 2D HSQC NMR spectrum (around 40-110/2.7-5.1 ppm) corresponded to the aryl alkyl ether structures (A). From these lignin subunits, A(OH), A(OEG) and A (RCOO) were assigned to aryl ether structures with OH groups linked at both  $\alpha$  and  $\gamma$  carbons (most likely from the native structure), aryl ether with grafted EG at the  $\alpha$  carbon (reaction of lignin with ES) and aryl ether with esterification at  $\gamma$  carbon, respectively (Figure 6b and Table S4). Taking in consideration the intensity of signals, it can be concluded that in OTP delignification using ChCl:pTSA:EG enables the isolation of a lignin fraction with some native-like (A(OH) subunits) macromolecular features, but a major fraction was grafted with EG molecules from ES into lignin structure (A(OEG)). This phenomenon was also reported in previous studies when using EG in presence of strong acids (oxalic and trifluoromethanesulfonic), where it is depicted the same  $^{13}\text{C}$ - $^1\text{H}$  cross assignments<sup>45,46</sup> in the analysis of lignin structure. An advantage of this chemical modification is the increased stability of the resulting lignin macromolecular structure. For instance, the formation of Hibbert Ketones, favored in acidic media, might be avoided during lignin extraction, since the reactive benzyl carbocations are trapped with ES molecules. This enables the isolation of lignin with less condensed structures.<sup>45,46</sup> Another feature of this lignin is the highly probable esterification of aryl ether subunits (A (RCOO) subunits), particularly with oleic acid, one of the most abundant long chain unsaturated fatty acids naturally present in OTP biomass (extractives fraction).<sup>47</sup> Strong oleic acid signals were identified in the aliphatic region of LIG-ES HSQC spectrum (Figure 6a), while esterification was confirmed by 2D HMBC cross signals, such as oleic acid carboxylate group coupling with  $\alpha$  carbon of aryl ether unit (through ester bond) as depicted in Figure 6d. Regarding to the aromatic region of the LIG-

ES HSQC spectrum (around 95-150/5.0-8.5 ppm), the presence of G- and S-type units from lignin is confirmed (Figure 6c).

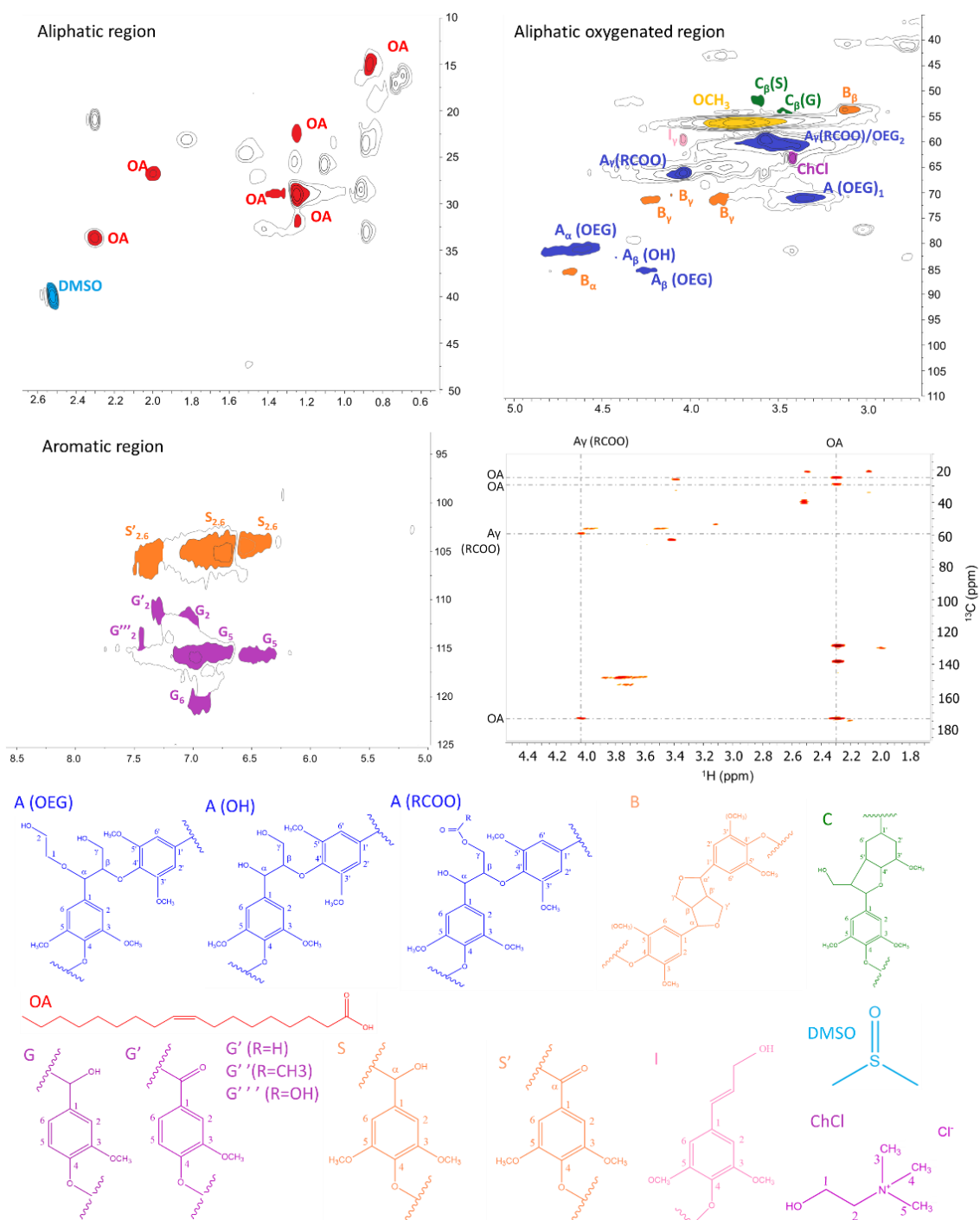


**Figure 6.** 2D HSQC and HMBC NMR of LIG-ES obtained after extraction with ChCl:pTSA:EG at 80 °C and 4 h. a) HSQC - aliphatic region; b) HSQC - aliphatic oxygenated

region; c) HSQC - aromatic region; d) HMBC showing  $^{13}\text{C}$ - $^1\text{H}$  cross signals between OA (Oleic acid) and  $\text{A}\gamma$  (aryl ether -  $\gamma$  carbon).

As mentioned before, the grafting of EG onto lignin structure decreases the occurrence of lignin condensation reactions.<sup>46</sup> This is also supported by TGA analysis (Figure S3a and Figure S3b), since the weight loss of LIG-ES is considerably higher when compared to the more condensed structure of Kraft lignin over the studied temperature range, in agreement with previously published data.<sup>48</sup>

On the other hand,  $^{31}\text{P}$  NMR analysis showed an impressive aliphatic OH content in LIG-ES sample, much higher than that observed for Kraft lignin (5.21 and 1.90  $\text{mmol}\cdot\text{g}^{-1}$  lignin, respectively) (Figure 7 and Figure S4). Once more, these results are in agreement to the grafting of EG onto lignin structure avoiding condensation reactions (usually decreases the OH content). Furthermore, the carboxylic acid content is also higher in LIG-ES, which may be associated to the presence of free (non-esterified) oleic acid and other unsaturated fatty acids that fall in the same chemical shift (134.92 ppm). Additionally, a clear difference in phenolic OH content can be seen by contrasting LIG-ES and Kraft lignins. The very harsh conditions of Kraft process enable the disruption of aryl ether structures producing phenolic units (6.58  $\text{mmol}\cdot\text{g}^{-1}$  lignin), while the milder conditions in the ternary ES treatment favor the grafting of EG to the detriment of the cleavage of  $\beta$ -O-4 bonds (2.67  $\text{mmol}\cdot\text{g}^{-1}$  lignin of phenolic OH groups).

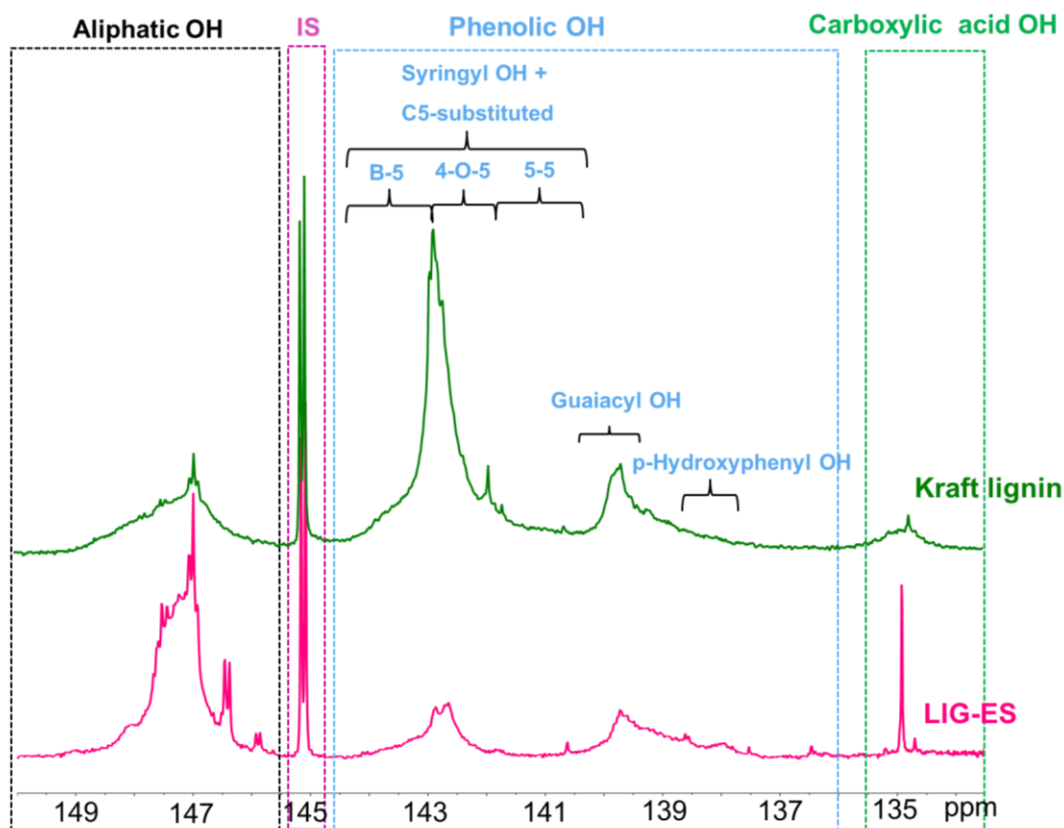


**Figure 7.** Quantitative  $^{31}\text{P}$  NMR spectra of LIG-ES after extraction with  $\text{ChCl:pTSA:EG}$  eutectic solvent (80 °C, 4 h) and Kraft lignin derivatized with TMDP using cyclohexanol as the internal standard (IS).

The molecular weight determination also demonstrated the benefit of protecting lignin macromolecules from condensation reactions with EG grafting. GPC data revealed that LIG-ES presents a average-weight molecular weight ( $M_w$ ) ( $9167 \text{ g}\cdot\text{mol}^{-1}$ ), almost an order magnitude higher than that of Kraft lignin ( $1520 \text{ g}\cdot\text{mol}^{-1}$ ).<sup>23</sup> However, the average-number molecular weight of LIG-ES was very low ( $1608 \text{ g}\cdot\text{mol}^{-1}$ ), (Table S5) resulting in a polydispersity index (PI) as high as 5.70, showcasing the heterogeneity of the isolated lignin that must be refined before application.

### 3.3. Ternary ES recovery to achieve process sustainability

ES recovery is an essential step that helps to complete the biomass delignification process in a sustainable and economically profitable way following the principles of green chemistry.<sup>7,49</sup> Purification steps as evaporation,<sup>7</sup> vacuum filtration,<sup>50</sup> freeze drying<sup>51</sup> and solid phase extraction (SPE)<sup>52</sup> have been reported for ES recovery and recycling. In the present study, after biomass delignification and lignin isolation steps, ternary ES was tentatively recovered by adsorption of impurities using a LiChroprep® RP-18 resin. As far as known, this setup was tested for the first time in the recovery of ES. After adsorption, around 90 % ES recovery yield was achieved, while the color exhibited by ES shifted from initial black to colorless and transparent recovered liquid, indicating an extensive removal of residual lignin and other impurities. The purification efficacy was further confirmed by <sup>1</sup>H and <sup>13</sup>C NMR analysis of the pristine ES, the ES submitted to process conditions without OTP biomass (80 °C and 4 h) and the recovered ES after adsorption. This sample rational was performed to elucidate upon the thermal stability of ES during delignification process, possible contaminations as well as deviations of molar proportions of ChCl:pTSA:EG after recovery step.

Figure 8 shows the <sup>1</sup>H NMR spectra of the three samples. No additional resonances were observed in the ES submitted to thermal processing at 80 °C or to the ES recovered after OTP fractionation process plus adsorption method, demonstrating that neither extraction conditions, biomass-ES reactions nor developed adsorption method affected the chemical composition of the recovered ES. Similar observations can be inferred from <sup>13</sup>C NMR spectra (Figure S5). Furthermore, the integration of the <sup>1</sup>H NMR resonances of recovered ES demonstrated ChCl:pTSA:EG with molar ratio of 1.07:1.02:8.96, which means that the ratios

of ES components were practically preserved after OTP fractionation and adsorption method, despite the grafting of EG onto lignin structure shown before. Indeed, a very low content of EG is expected to be lost from ES, since the mass of extracted lignin represents approximately 1.25 % of ES total mass used in OTP delignification.

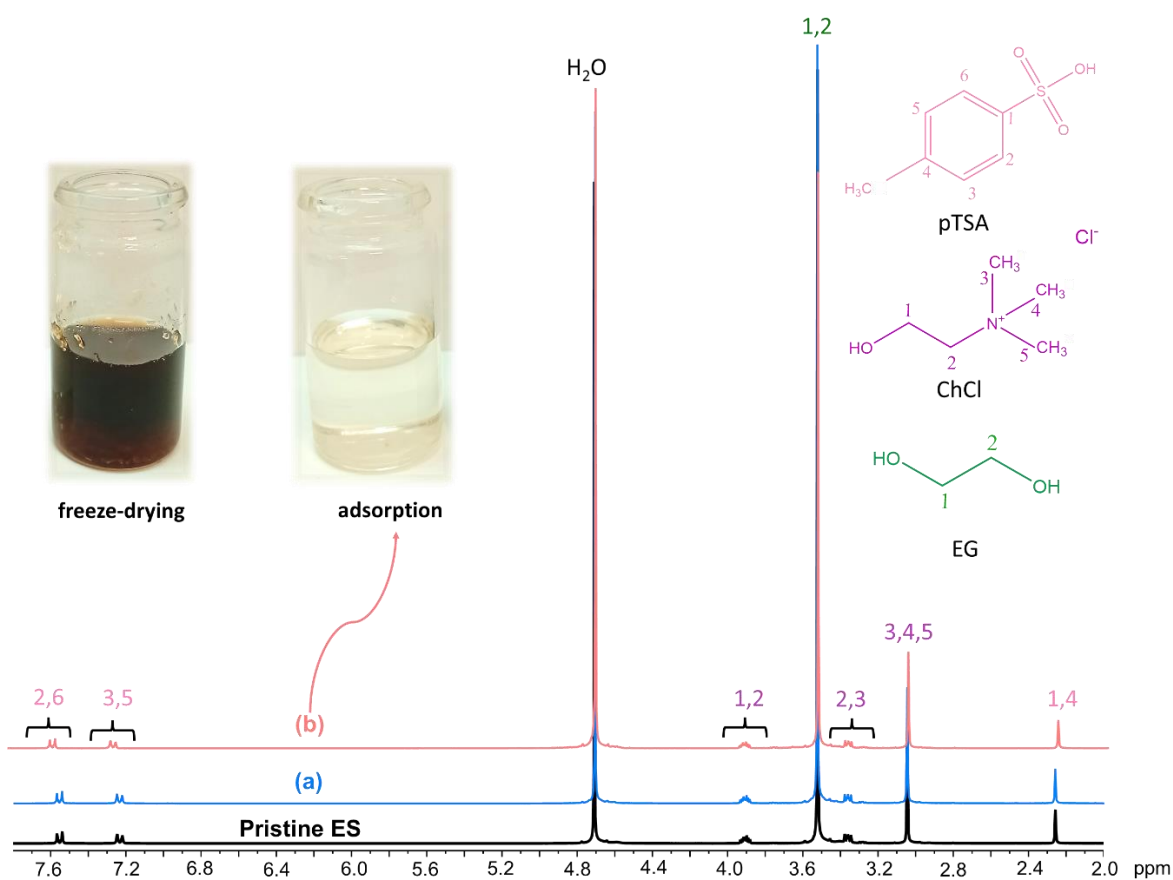


**Figure 8.**  $^1\text{H}$  NMR spectra for pristine ES (after thermal heating at 80 °C and 4 h), as well as recovered ES obtained after OTP fractionation (a) and adsorption (b). Images of ES before and after adsorption are presented.

#### 4. CONCLUSIONS

This work disclosed a comprehensive study on the efficiency of ChCl:pTSA:EG (1:1:9) in the fractionation and valorization of olive tree pruning (OTP) biomass. The results obtained

from the characterization of both separated fractions of cellulose (S-ES) and lignin (LIG-ES) achieved in this study show that ternary ChCl:PTSA:EG is a promising solvent for OTP fractionation. The application of this ternary ES (ChCl:pTSA:EG) at 80 °C and 4 h achieved the highest lignin extraction (62.7 %) and hemicellulose removal (87.3 %), allowing cellulose enrichment in the resulting solid (S-ES) and providing more accessibility to cellulases (cellulose saccharification up to 81.8 % -  $\text{g}_{\text{glucan}} \cdot 100 \text{ g}^{-1}_{\text{glucan OTP}}$ ). In addition, the isolated lignin (LIG-ES) revealed unique characteristics due to EG grafting onto lignin macromolecules, providing a high content of aliphatic OH groups (5.2 mmol·g<sup>-1</sup> lignin). This phenomenon provides chemical functionality to the isolated lignin that may favor its application as starting material for new bio-based material synthesis, nanotechnology, cosmetics, nutraceuticals or other specialized applications. Finally, ES can be successfully regenerated by applying a new and simple adsorption method capable of removing residual lignin and other impurities after biomass fractionation process. Forward work should rely on the optimization and scale-up activities of this OTP fractionation process.

## **SUPPORTING INFORMATION**

Details on used reagents, chemical composition of solid and liquid fractions, FTIR, TGA, 31P NMR and GPC data of LIG-ES, <sup>13</sup>C NMR data of eutectic solvents, as well as FTIR and 2D HSQC assignments (PDF).

## **ACKNOWLEDGMENTS**

This work was developed within the scope of the project CICECO-Aveiro Institute of Materials, UIDB/50011/2020, UIDP/50011/2020 & LA/P/0006/2020, financed by national funds through the FCT/MCTES (PIDDAC). I. Gómez-Cruz expresses her gratitude to the

University of Jaén and the Ministry of Universities for the financial support of the Grants for the Recalibration of the Spanish University System for 2021-2023 in the Margarita Salas modality for the training of young doctors. André M. da Costa Lopes thanks his research contract funded by Fundação para a Ciência e Tecnologia (FCT) and project CENTRO-04-3559-FSE-000095 - Centro Portugal Regional Operational Programme (Centro2020), under the PORTUGAL 2020 Partnership Agreement, through the European Regional Development Fund (ERDF). National NMR Network, funded within the framework of the National Program for Scientific Re-equipment, contract REDE/1517/RMN/2005 with funds from POCI 2010 (FEDER) and FCT.

## REFERENCES

- (1) Ashokkumar, V.; Venkatkarthick, R.; Jayashree, S.; Chuetor, S.; Dharmaraj, S.; Kumar, G.; Chen, W. H.; Ngamcharussrivichai, C. Recent Advances in Lignocellulosic Biomass for Biofuels and Value-Added Bioproducts - A Critical Review. *Bioresour. Technol.* **2022**, *344* (126195). <https://doi.org/10.1016/j.biortech.2021.126195>.
- (2) Gómez-Cruz, I.; Cara, C.; Romero, I.; Castro, E.; Gullón, B. Valorisation of Exhausted Olive Pomace by an Ecofriendly Solvent Extraction Process of Natural Antioxidants. *Antioxidants* **2020**, *9* (1010), 1–18. <https://doi.org/10.3390/antiox9101010>.
- (3) Liu, B.; Liu, J.; Huang, D.; Pei, D.; Wei, J.; Di, D. Isolation and Purification of Oleuropein from Olive Leaves Using Boric Acid Affinity Resin and a Novel Solvent System. *Colloids Surfaces A Physicochem. Eng. Asp.* **2021**, *614*, (126145). <https://doi.org/10.1016/j.colsurfa.2021.126145>.
- (4) Martínez-Patiño, J. C.; Romero-García, J. M.; Ruiz, E.; Oliva, J. M.; Álvarez, C.;

- Romero, I.; Negro, M. J.; Castro, E. High Solids Loading Pretreatment of Olive Tree Pruning with Dilute Phosphoric Acid for Bioethanol Production by *Escherichia Coli*. *Energy and Fuels* **2015**, *29*, 1735–1742. <https://doi.org/10.1021/ef502541r>.
- (5) Contreras, M. del M.; Romero, I.; Moya, M.; Castro, E. Olive-Derived Biomass as a Renewable Source of Value-Added Products. *Process Biochem.* **2020**, *97*, 43–56. <https://doi.org/10.1016/j.procbio.2020.06.013>.
- (6) Romero-García, J. M.; López-Linares, J. C.; Contreras, M. del M.; Romero, I.; Castro, E. Exploitation of Olive Tree Pruning Biomass through Hydrothermal Pretreatments. *Ind. Crops Prod.* **2022**, *176* (114425). <https://doi.org/10.1016/j.indcrop.2021.114425>.
- (7) Chen, Z.; Ragauskas, A.; Wan, C. Lignin Extraction and Upgrading Using Deep Eutectic Solvents. *Ind. Crops Prod.* **2020**, *147* (112241). <https://doi.org/10.1016/j.indcrop.2020.112241>.
- (8) Fonseca, B. G.; Mateo, S.; Roberto, I. C.; Sánchez, S.; Moya, A. J. Bioconversion in Batch Bioreactor of Olive-Tree Pruning Biomass Optimizing Treatments for Ethanol Production. *Biochem. Eng. J.* **2020**, *164* (107793). <https://doi.org/10.1016/j.bej.2020.107793>.
- (9) Zhou, M.; Fakayode, O. A.; Ahmed Yagoub, A. E. G.; Ji, Q.; Zhou, C. Lignin Fractionation from Lignocellulosic Biomass Using Deep Eutectic Solvents and Its Valorization. *Renew. Sustain. Energy Rev.* **2022**, *156* (111986). <https://doi.org/10.1016/j.rser.2021.111986>.
- (10) Gosselink, R. J. A. Lignin as a Renewable Aromatic Resource for the Chemical Industry, 2011.
- (11) Gómez-Cruz, I.; Contreras, M. del M.; Romero, I.; Castro, E. A Biorefinery Approach to Obtain Antioxidants, Lignin and Sugars from Exhausted Olive Pomace. *J. Ind. Eng.*

- Chem.* **2021**, *96*, 356–363. <https://doi.org/10.1016/j.jiec.2021.01.042>.
- (12) Garlapati, V. K.; Chandel, A. K.; Kumar, S. P. J.; Sharma, S.; Sevda, S.; Ingle, A. P.; Pant, D. Circular Economy Aspects of Lignin: Towards a Lignocellulose Biorefinery. *Renew. Sustain. Energy Rev.* **2020**, *130* (109977). <https://doi.org/10.1016/j.rser.2020.109977>.
- (13) Zhu, J.; Yan, C.; Zhang, X.; Yang, C.; Jiang, M.; Zhang, X. A Sustainable Platform of Lignin: From Bioresources to Materials and Their Applications in Rechargeable Batteries and Supercapacitors. *Prog. Energy Combust. Sci.* **2020**, *76*, 100788. <https://doi.org/10.1016/j.pecs.2019.100788>.
- (14) Gutiérrez-Villanueva, A.; Guirola Céspedes, C.; de Armas Martínez, A. C.; Albernas Carvajal, Y.; Villanueva Ramos, G. Valorización de La Lignina En El Concepto de Biorrefinería (I). *Cent. Azúcar* **2020**, *47* (3), 95–105.
- (15) Toledano, A.; Serrano, L.; Labidi, J. Enhancement of Lignin Production from Olive Tree Pruning Integrated in a Green Biorefinery. *Ind. Eng. Chem. Res.* **2011**, *50*, 6573–6579. <https://doi.org/10.1021/ie102142f>.
- (16) Erdocia, X.; Prado, R.; Corcuera, M. Á.; Labidi, J. Effect of Different Organosolv Treatments on the Structure and Properties of Olive Tree Pruning Lignin. *J. Ind. Eng. Chem.* **2014**, *20*, 1103–1108. <https://doi.org/10.1016/j.jiec.2013.06.048>.
- (17) Eugenio, M. E.; Martín-Sampedro, R.; Santos, J. I.; Wicklein, B.; Ibarra, D. Chemical, Thermal and Antioxidant Properties of Lignins Solubilized during Soda/AQ Pulp of Orange and Olive Tree Pruning Residues. *Molecules* **2021**, *26* (3819).
- (18) Santos, J. I.; Martín-Sampedro, R.; Fillat, Ú.; Oliva, J. M.; Negro, M. J.; Ballesteros, M.; Eugenio, M. E.; Ibarra, D. Evaluating Lignin-Rich Residues from Biochemical Ethanol Production of Wheat Straw and Olive Tree Pruning by FTIR and 2D-NMR.

*Int. J. Polym. Sci.* **2015**, 2015. <https://doi.org/10.1155/2015/314891>.

- (19) Santos, J. I.; Fillat, Ú.; Martín-Sampedro, R.; Eugenio, M. E.; Negro, M. J.; Ballesteros, I.; Rodríguez, A.; Ibarra, D. Evaluation of Lignins from Side-Streams Generated in an Olive Tree Pruning-Based Biorefinery: Bioethanol Production and Alkaline Pulping. *Int. J. Biol. Macromol.* **2017**, *105*, 238–251. <https://doi.org/10.1016/j.ijbiomac.2017.07.030>.
- (20) Kohli, K.; Katuwal, S.; Biswas, A.; Sharma, B. K. Effective Delignification of Lignocellulosic Biomass by Microwave Assisted Deep Eutectic Solvents. *Bioresour. Technol.* **2020**, *303* (122897). <https://doi.org/10.1016/j.biortech.2020.122897>.
- (21) Zhang, M.; Zhang, X.; Liu, Y.; Wu, K.; Zhu, Y.; Lu, H.; Liang, B. Insights into the Relationships between Physicochemical Properties, Solvent Performance, and Applications of Deep Eutectic Solvents. *Environ. Sci. Pollut. Res.* **2021**, *28*, 35537–35563. <https://doi.org/10.1007/s11356-021-14485-2>.
- (22) Abad-Gil, L.; Procopio, J. R.; Brett, C. M. A. Binary and Ternary Deep Eutectic Solvent Mixtures: Influence on Methylene Blue Electropolymerisation. *Electrochem. commun.* **2021**, *124* (106967). <https://doi.org/10.1016/j.elecom.2021.106967>.
- (23) Sosa, F. H. B.; Abranches, D. O.; Da Costa Lopes, A. M.; Coutinho, J. A. P.; Da Costa, M. C. Kraft Lignin Solubility and Its Chemical Modification in Deep Eutectic Solvents. *ACS Sustain. Chem. Eng.* **2020**, *8*, 18577–18589. <https://doi.org/10.1021/acssuschemeng.0c06655>.
- (24) Soares, B.; Tavares, D. J. P.; Amaral, J. L.; Silvestre, A. J. D.; Freire, C. S. R.; Coutinho, J. A. P. Enhanced Solubility of Lignin Monomeric Model Compounds and Technical Lignins in Aqueous Solutions of Deep Eutectic Solvents. *ACS Sustain. Chem. Eng.* **2017**, *5* (5), 4056–4065. <https://doi.org/10.1021/acssuschemeng.7b00053>.

- (25) Smink, D.; Juan, A.; Schuur, B.; Kersten, S. R. A. Understanding the Role of Choline Chloride in Deep Eutectic Solvents Used for Biomass Delignification. *Ind. Eng. Chem. Res.* **2019**, *58*, 16348–16357. <https://doi.org/10.1021/acs.iecr.9b03588>.
- (26) Da Costa Lopes, A. M.; Gomes, J. R. B.; Coutinho, J. A. P.; Silvestre, A. J. D. Novel Insights into Biomass Delignification with Acidic Deep Eutectic Solvents: A Mechanistic Study of  $\beta$ -O-4 Ether Bond Cleavage and the Role of the Halide Counterion in the Catalytic Performance. *Green Chem.* **2020**, *22*, (2474). <https://doi.org/10.1039/c9gc02569c>.
- (27) Poy, H.; da Costa Lopes, A. M.; Lladosa, E.; Gabaldón, C.; Loras, S.; Silvestre, A. J. D. Enhanced Biomass Processing towards Acetone-Butanol-Ethanol Fermentation Using a Ternary Deep Eutectic Solvent. *Renew. Energy* **2023**, *219*, 119488. <https://doi.org/10.1016/j.renene.2023.119488>.
- (28) Yang, J. Y.; Guo, T. S.; Xu, Y. H.; Li, M. F.; Bian, J. Structure and Properties of Eucalyptus Lignin Extracted with Benzenesulfonic and  $\rho$ -Toluenesulfonic Acids under Mild Conditions. *Ind. Crops Prod.* **2023**, *194* (116269). <https://doi.org/10.1016/j.indcrop.2023.116269>.
- (29) Soares, B.; Silvestre, A. J. D.; Rodrigues Pinto, P. C.; Freire, C. S. R.; Coutinho, J. A. P. Hydrotrophy and Cosolvency in Lignin Solubilization with Deep Eutectic Solvents. *ACS Sustain. Chem. Eng.* **2019**, *7* (14), 12485–12493. <https://doi.org/10.1021/acssuschemeng.9b02109>.
- (30) Sluiter, A.; Hames, B.; Ruiz, R.; Scarlata, C.; Sluiter, J.; Templeton, D.; Crocker, D. *Determination of Structural Carbohydrates and Lignin in Biomass*, **2012**, NREL/TP-510-42618.
- (31) Rencoret, J.; Gutiérrez, A.; Castro, E.; del Ró, J. C. Structural Characteristics of Lignin

- in Pruning Residues of Olive Tree (*Olea Europaea L.*). *Holzforschung* **2019**, *73* (1), 25–34.
- (32) Oh, Y.; Park, S.; Jung, D.; Oh, K. K.; Lee, S. H. Effect of Hydrogen Bond Donor on the Choline Chloride-Based Deep Eutectic Solvent-Mediated Extraction of Lignin from Pine Wood. *Int. J. Biol. Macromol.* **2020**, *165*, 187–197. <https://doi.org/10.1016/j.ijbiomac.2020.09.145>.
- (33) Hou, X. D.; Feng, G. J.; Ye, M.; Huang, C. M.; Zhang, Y. Significantly Enhanced Enzymatic Hydrolysis of Rice Straw via a High-Performance Two-Stage Deep Eutectic Solvents Synergistic Pretreatment. *Bioresour. Technol.* **2017**, *238*, 139–146. <https://doi.org/10.1016/j.biortech.2017.04.027>.
- (34) Zhai, Q.; Long, F.; Jiang, X.; Hse, C. yun; Jiang, J.; Xu, J. Facile and Rapid Fractionation of Bamboo Wood with a P-Toluenesulfonic Acid-Based Three-Constituent Deep Eutectic Solvent. *Ind. Crops Prod.* **2020**, *158* (113018). <https://doi.org/10.1016/j.indcrop.2020.113018>.
- (35) Alañón, M. E.; Ivanović, M.; Gómez-Caravaca, A. M.; Arráez-Román, D.; Segura-Carretero, A. Choline Chloride Derivative-Based Deep Eutectic Liquids as Novel Green Alternative Solvents for Extraction of Phenolic Compounds from Olive Leaf. *Arab. J. Chem.* **2020**, *13*, 1685–1701. <https://doi.org/10.1016/j.arabjc.2018.01.003>.
- (36) Cao, Q.; Li, J.; Xia, Y.; Li, W.; Luo, S.; Ma, C.; Liu, S. Green Extraction of Six Phenolic Compounds from Rattan (*Calamoideae Faberii*) with Deep Eutectic Solvent by Homogenate-Assisted Vacuum-Cavitation Method. *Molecules* **2019**, *24* (113). <https://doi.org/10.3390/molecules24010113>.
- (37) López-Linares, J. C.; Romero-García, J. M.; Romero, I.; Ruiz, E.; Castro, E. Development of a Biorefinery from Olive Mill Leaves: Comparison of Different

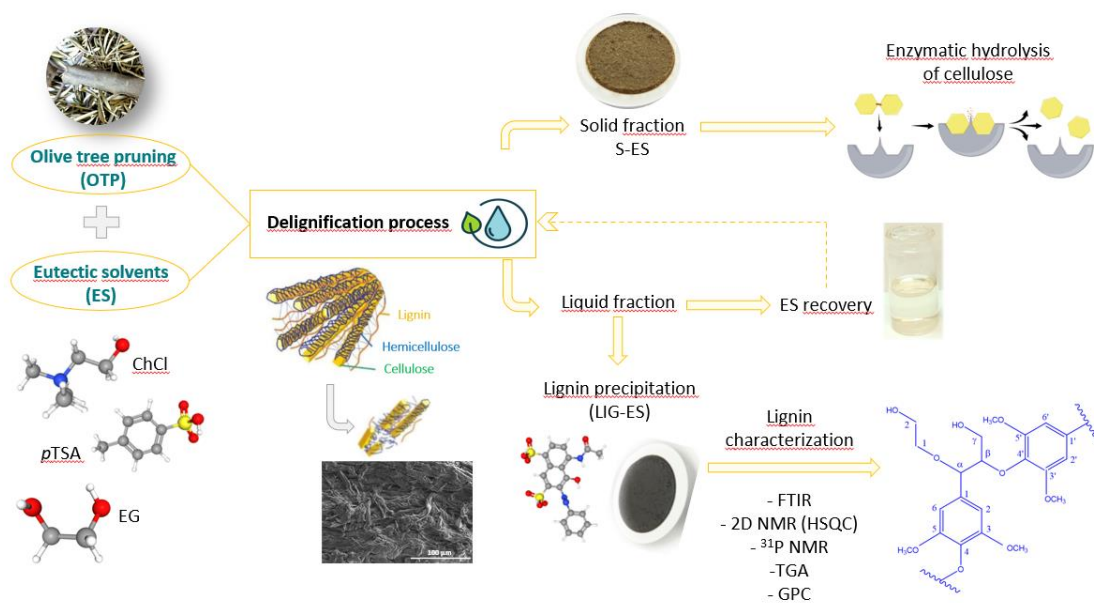
- Process Configurations. *Ind. Crops Prod.* **2023**, *200* (116813).  
<https://doi.org/10.1016/j.indcrop.2023.116813>.
- (38) Ballesteros, I.; Ballesteros, M.; Cara, C.; Sáez, F.; Castro, E.; Manzanares, P.; Negro, M. J.; Oliva, J. M. Effect of Water Extraction on Sugars Recovery from Steam Exploded Olive Tree Pruning. *Bioresour. Technol.* **2011**, *102*, 6611–6616.  
<https://doi.org/10.1016/j.biortech.2011.03.077>.
- (39) Saini, J. K.; Patel, A. K.; Adsul, M.; Singhanian, R. R. Cellulase Adsorption on Lignin: A Roadblock for Economic Hydrolysis of Biomass. *Renew. Energy* **2016**, *98*, 29–42.  
<https://doi.org/10.1016/j.renene.2016.03.089>.
- (40) Miliotti, E.; Dell’Orco, S.; Lotti, G.; Rizzo, A. M.; Rosi, L.; Chiaramonti, D. Lignocellulosic Ethanol Biorefinery: Valorization of Lignin-Rich Stream through Hydrothermal Liquefaction. *Energies* **2019**, *12* (723).  
<https://doi.org/10.3390/en12040723>.
- (41) Yang, Y.; Zhao, L.; Ren, J.; He, B. Effect of Ternary Deep Eutectic Solvents on Bagasse Cellulose and Lignin Structure in Low-Temperature Pretreatment. *Processes* **2022**, *10* (778). <https://doi.org/10.3390/pr10040778>.
- (42) Chen, Z.; Jacoby, W. A.; Wan, C. Ternary Deep Eutectic Solvents for Effective Biomass Deconstruction at High Solids and Low Enzyme Loadings. *Bioresour. Technol.* **2019**, *279*, 281–286. <https://doi.org/10.1016/j.biortech.2019.01.126>.
- (43) Bock, P.; Nousiainen, P.; Elder, T.; Blaukopf, M.; Amer, H.; Zirbs, R.; Potthast, A.; Gierlinger, N. Infrared and Raman Spectra of Lignin Substructures: Dibenzodioxocin. *J. Raman Spectrosc.* **2020**, *51*, 422–431. <https://doi.org/10.1002/jrs.5808>.
- (44) Joffres, B.; Lorentz, C.; Vidalie, M.; Laurenti, D.; Quoineaud, A. A.; Charon, N.; Daudin, A.; Quignard, A.; Geantet, C. Catalytic Hydroconversion of a Wheat Straw

- Soda Lignin: Characterization of the Products and the Lignin Residue. *Appl. Catal. B Environ.* **2014**, *145*, 167–176. <https://doi.org/10.1016/j.apcatb.2013.01.039>.
- (45) Wang, Z.; Liu, Y.; Barta, K.; Deuss, P. J. The Effect of Acidic Ternary Deep Eutectic Solvent Treatment on Native Lignin. *ACS Sustain. Chem. Eng.* **2022**, *10*, 12569–12579. <https://doi.org/10.1021/acssuschemeng.2c02954>.
- (46) Liu, Y.; Deak, N.; Wang, Z.; Yu, H.; Hameleers, L.; Jurak, E.; Deuss, P. J.; Barta, K. Tunable and Functional Deep Eutectic Solvents for Lignocellulose Valorization. *Nat. Commun.* **2021**, *12* (5424). <https://doi.org/10.1038/s41467-021-25117-1>.
- (47) Gullón, B.; Gullón, P.; Eibes, G.; Cara, C.; De Torres, A.; López-Linares, J. C.; Ruiz, E.; Castro, E. Valorisation of Olive Agro-Industrial by-Products as a Source of Bioactive Compounds. *Sci. Total Environ.* **2018**, *645*, 533–542. <https://doi.org/10.1016/j.scitotenv.2018.07.155>.
- (48) Choi, J. H.; Cho, S. M.; Kim, J. C.; Park, S. W.; Cho, Y. M.; Koo, B.; Kwak, H. W.; Choi, I. G. Thermal Properties of Ethanol Organosolv Lignin Depending on Its Structure. *ACS Omega* **2021**, *6* (2), 1534–1546. <https://doi.org/10.1021/acsomega.0c05234>.
- (49) Zhang, M.; Tian, R.; Tang, S.; Wu, K.; Wang, B.; Liu, Y.; Zhu, Y.; Lu, H.; Liang, B. Multistage Treatment of Bamboo Powder Waste Biomass: Highly Efficient and Selective Isolation of Lignin Components. *Waste Manag.* **2023**, *166*, 35–45. <https://doi.org/10.1016/j.wasman.2023.04.040>.
- (50) Mamilla, J. L. K.; Novak, U.; Grilc, M.; Likozar, B. Natural Deep Eutectic Solvents (DES) for Fractionation of Waste Lignocellulosic Biomass and Its Cascade Conversion to Value-Added Bio-Based Chemicals. *Biomass and Bioenergy* **2019**, *120*, 417–425. <https://doi.org/10.1016/j.biombioe.2018.12.002>.

- (51) Jeong, K. M.; Lee, M. S.; Nam, M. W.; Zhao, J.; Jin, Y.; Lee, D. K.; Kwon, S. W.; Jeong, J. H.; Lee, J. Tailoring and Recycling of Deep Eutectic Solvents as Sustainable and Efficient Extraction Media. *J. Chromatogr. A* **2015**, *1424*, 10–17. <https://doi.org/10.1016/j.chroma.2015.10.083>.
- (52) Isci, A.; Kaltschmitt, M. Recovery and Recycling of Deep Eutectic Solvents in Biomass Conversions: A Review. *Biomass Convers. Biorefinery* **2022**, *12 (Suppl 1)*, S197–S226. <https://doi.org/10.1007/s13399-021-01860-9>.

## SYNOPSIS

“For Table of Contents Only”



Fractionation of olive tree pruning assisted by a ternary eutectic solvent into isolated fractions of cellulose and lignin with unique functionality.